

# Next Generation Regional Arrays for Strong and Weak Motion using Cascadia 120 Slim Posthole

Geoffrey Bainbridge (Nanometrics) [geoffreybainbridge@nanometrics.ca](mailto:geoffreybainbridge@nanometrics.ca), Alex Chun-Chang Chen (UB Union), Tim Parker (Nanometrics), Daniela Wuthrich (Nanometrics), Yin Li (Nanometrics), Nick Pelyk (Nanometrics)

## ABSTRACT

Existing regional and EEW networks can be improved in data quality, providing more stations with unclipped continuous waveform observations and a uniform magnitude of completeness (Mc). This is possible using upgraded deeper sensor emplacements and new instrumentation, based on a current understanding of system noise and updated equipment available today. Station density is increasing with the US EEW buildout, with a focus on minimizing latency, which also presents an opportunity to improve data quality for weak motion. Mc and signal-to-noise ratio across the seismic and geodetic spectrum will be important for future OEF challenges and for hazard and science efforts such as 4D studies and the proposed new plate boundary type observatories, SZ4D and RuFZO. Recent development of network Mc simulation code by the USGS (Wilson et al., 2021) can be used to plan new networks, or infill stations to economically upgrade existing networks to these new best practices.

An instrument system that provides high-gain weak motion data in precise alignment with strong motion data at a single point in bedrock allows combined processing to create a seamless data set with maximum dynamic range. The Nanometrics Cascadia 120 Slim Posthole has been designed to meet these requirements. Both weak and strong motion sensors are integrated in a single case which enables lowest system noise, unclipped observations, and precise coherence of signals between the weak and strong motion channels. Cascadia 120 Slim and Cascadia Compact are deployed in networks now and we present data showing the noise floor for weak motion, a seamless transition to strong motion, and high coherence between the two sensors for mid-sized events.

## Cascadia Overview

Nanometrics Cascadia product line (shown in Figure 1 below) provides options to combine a Titan Class A strong motion accelerometer with various models of Trillium weak motion broadband seismometers in a single package so their outputs are mutually aligned.

- Cascadia Compact PH combines Titan with Trillium Compact in a 97 mm diameter unit for monitoring of local and regional seismicity with minimum size, power, and cost.
- The new Cascadia 120 Slim PH combines Titan with Trillium 120 Slim in a 104 mm diameter unit able to capture the full dynamic range of seismic ground motion from 4g to NLNM background noise (see Figure 3).
- The Cascadia Integration Kit attaches a Titan Posthole seismometer on top of a Trillium 120 Posthole or Borehole seismometer (diameter 143 mm) to add strong motion capability to an existing broadband station. It is also compatible with Trillium 360 Posthole or Borehole (diameter 146 mm) to enable the maximum possible dynamic range at low frequencies.

All these are designed for downhole deployment with up to 300 m water immersion, or 500 m in a dry borehole. Placing the sensors in high velocity bedrock minimizes latency for earthquake early warning, and minimizes site noise and surface layer resonances. Figure 2 shows a schematic diagram of a cased borehole installation. The borehole need not be deep if bedrock is close to surface. The wellhead can be used as a geodetic GNSS monument as per Williams (2010) so a single cased hole can efficiently host three instruments. Cascadia instruments are also suitable for direct burial, providing an efficient option for temporary or long-term deployment.

Figure 1: Cascadia product line (approximately to scale)

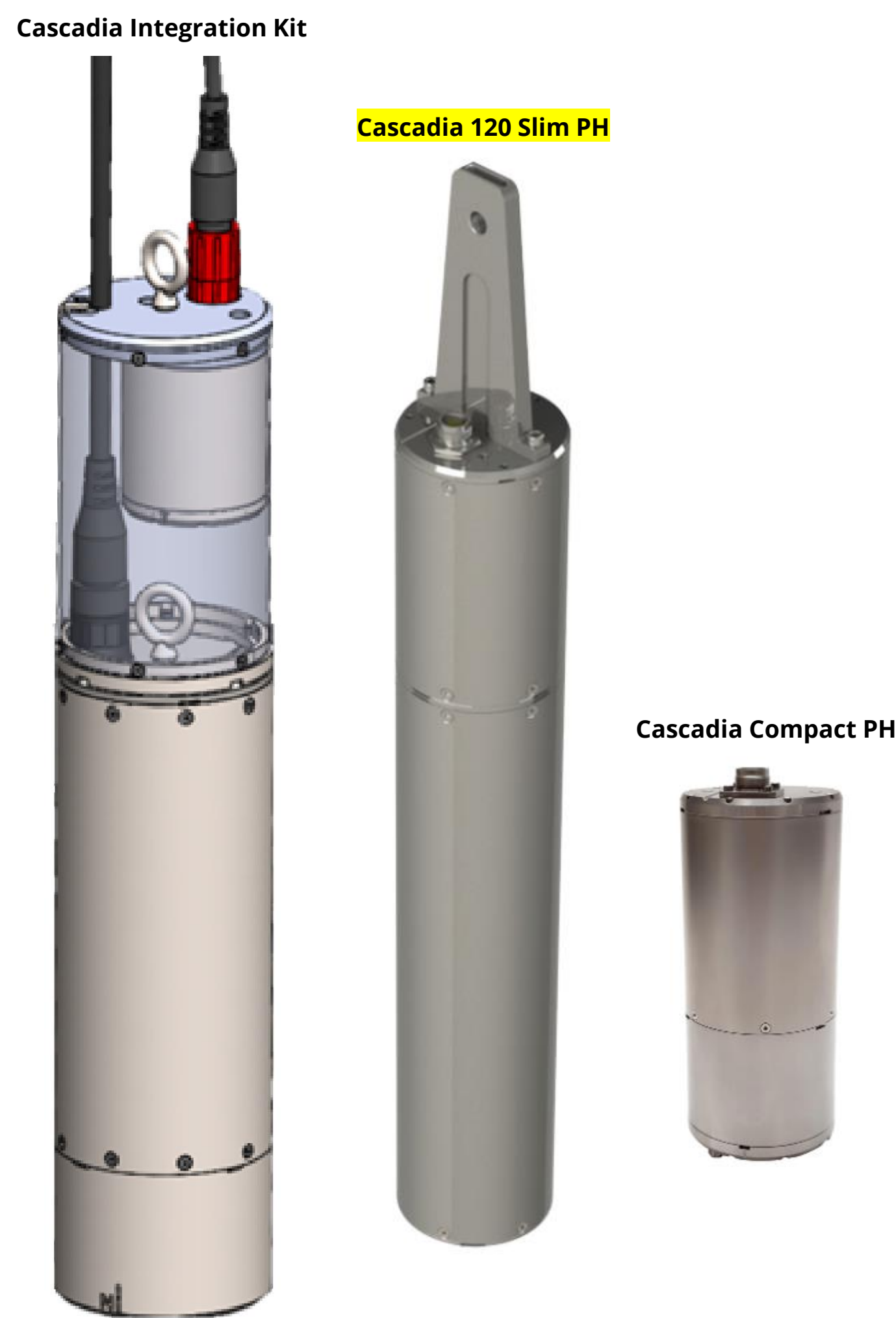
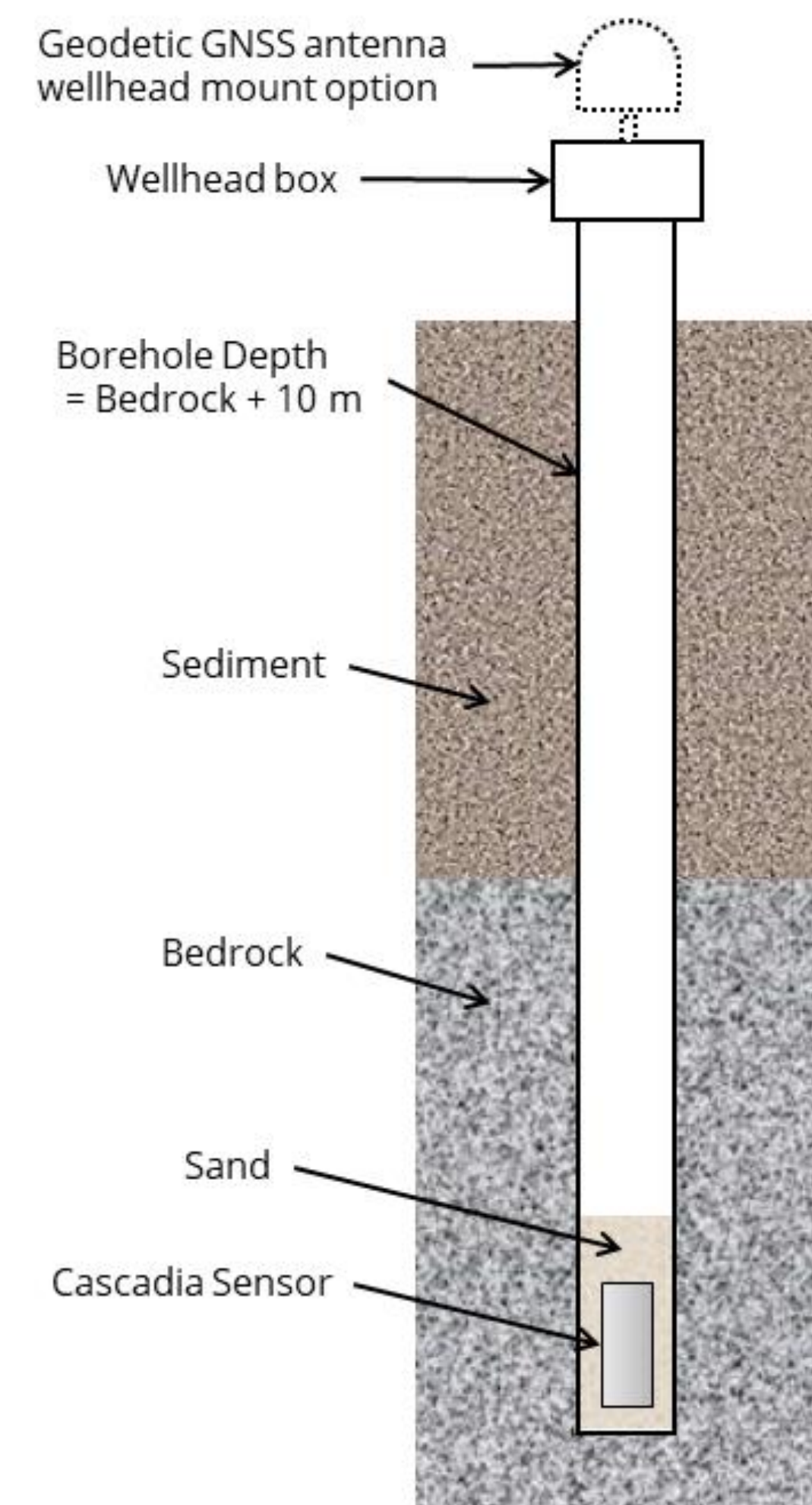


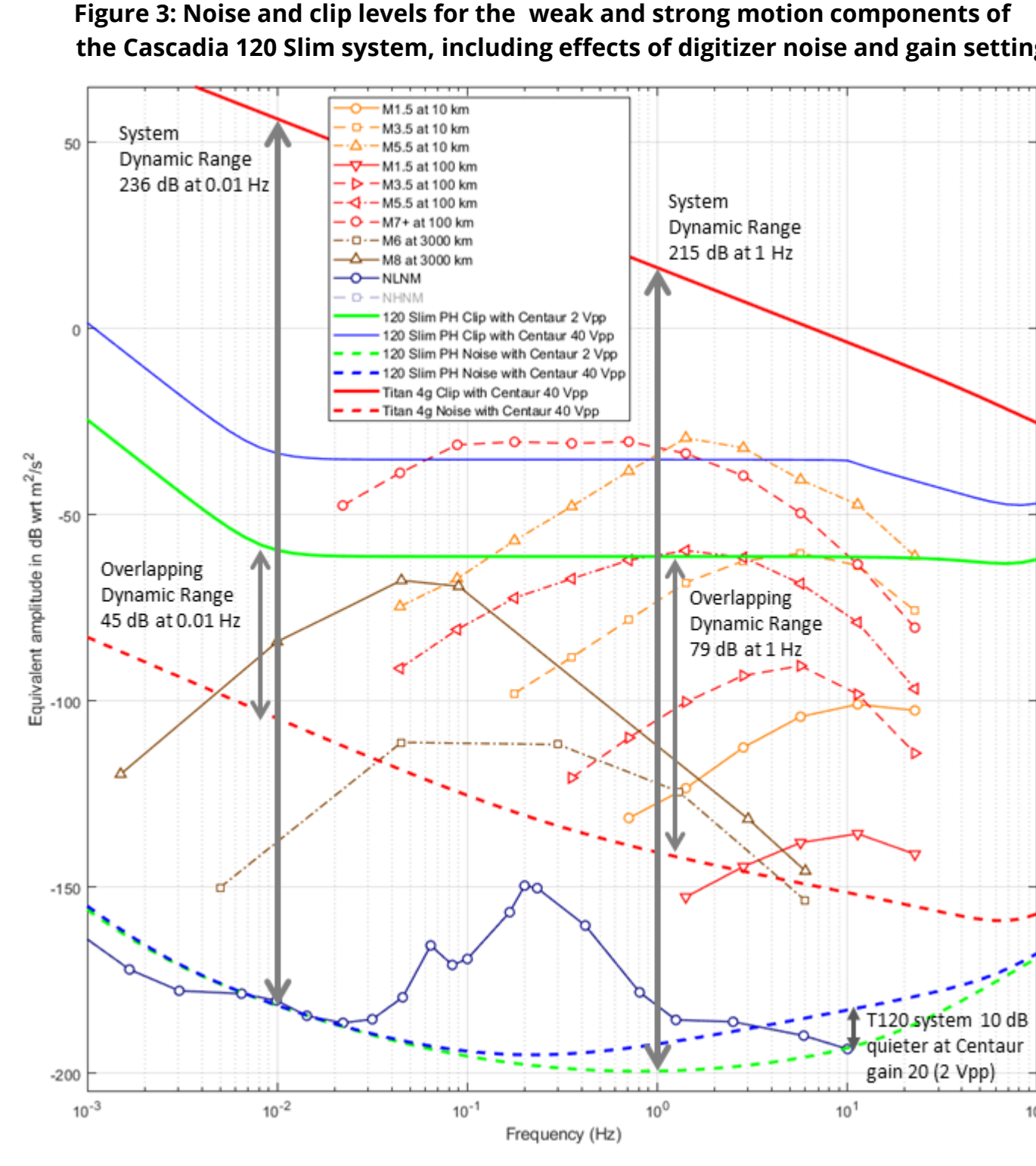
Figure 2: Example borehole design for Cascadia multi-sensor early warning + scientific networks



## Maximizing Dynamic Range

Cascadia 120 Slim PH provides a unique capability to resolve the entire dynamic range and frequency spectrum of seismic ground motion. Traditionally, strong and weak motion studies have been somewhat separate domains, in part because of the lack of a single instrument to capture both. Even for a single strong or weak motion sensor, some of its dynamic range is lost because of digitizer limitations. However, combining strong and weak motion sensors with overlapping dynamic range allows an optimization, where the weak motion digitizer gain can be increased to capture the noise floor of the seismometer, without giving up the high end of its range because that is covered by the strong motion system. Similarly, the strong motion system can be set to its maximum range of 4g because its noise floor is covered by the weak motion system.

Figure 3 shows clip level and noise in units of peak velocity in 1-octave bandwidth for Titan in 4g mode with digitizer gain 1 (red lines) and for T120 Slim PH with digitizer gain 20, 2 Vpp (green lines). Total dynamic range is a remarkable 215 dB at 1 Hz and 236 dB at 0.01 Hz. Their overlapping range is 79 dB at 1 Hz and 45 dB at 0.01 Hz. Note the spectra of many commonly observed earthquake events fall in this overlap range. The blue lines show noise and clip for T120 Slim PH with digitizer gain 1 (40 Vpp) which creates more overlap, but raises the noise floor at 10 Hz, so gain 20 (2 Vpp) seems more optimal.



## Case Study: Taiwan Downhole Seismic Observation Network

In Taiwan, UB Union is currently deploying Cascadia 120 Slim in the Downhole Seismic Observation Network of the Central Weather Bureau Seismological Center, for earthquake early warning and better understanding of blind fault systems. The instruments are sand installed in 200 to 400 m deep boreholes, in order to reach high-velocity bedrock, minimize latency for early warning, and maximize signal to noise ratio for continuous scientific data. Initial results show the high dynamic range of the instrument and coherence between the weak and strong motion signals which enables the two data streams to be seamlessly combined during earthquake events, as detailed in the following section at right regarding the Yilan earthquake.

Figure 5 (below right) shows the acceleration power spectral density (PSD) of background noise at a typical station, SSPB at Xin Pi. (Note these are different units than in the dynamic range plot above.) Signal from the Cascadia seismometer is shown by the solid red line, and from the accelerometer in dotted red. The signals are the same at frequencies above 0.2 Hz, where the microseismic peak rises above the noise floor of the strong motion accelerometer system. At lower frequencies the seismometer records lower levels of ground motion signal, approaching the NLNM at 0.01 Hz on Z (vertical channel), but the strong motion system is limited by its noise floor as expected.

The expected self-noise floor of the strong motion accelerometer system is shown by the dashed purple line. This is set by the noise of the digitizer rather than the accelerometer itself. (Because the strong motion instrument necessarily has lower sensitivity than the weak motion seismometer, it puts a smaller signal into the digitizer for the same ground motion, and the noise of the digitizer becomes a limiting factor when the signal is very small.)

The difference between the seismometer and accelerometer signals is shown by the light blue line. This matches with the expected noise floor of the accelerometer system, because this noise is the cause of the difference. The noise of the seismometer is much lower and does not contribute significantly to the difference. Because the seismometer and accelerometer are precisely calibrated and aligned together, there is no significant difference in their measurements of the microseismic peak ground motion, so this also does not contribute to the difference signal.

Figure 4: Map of existing CWB Seismic Network

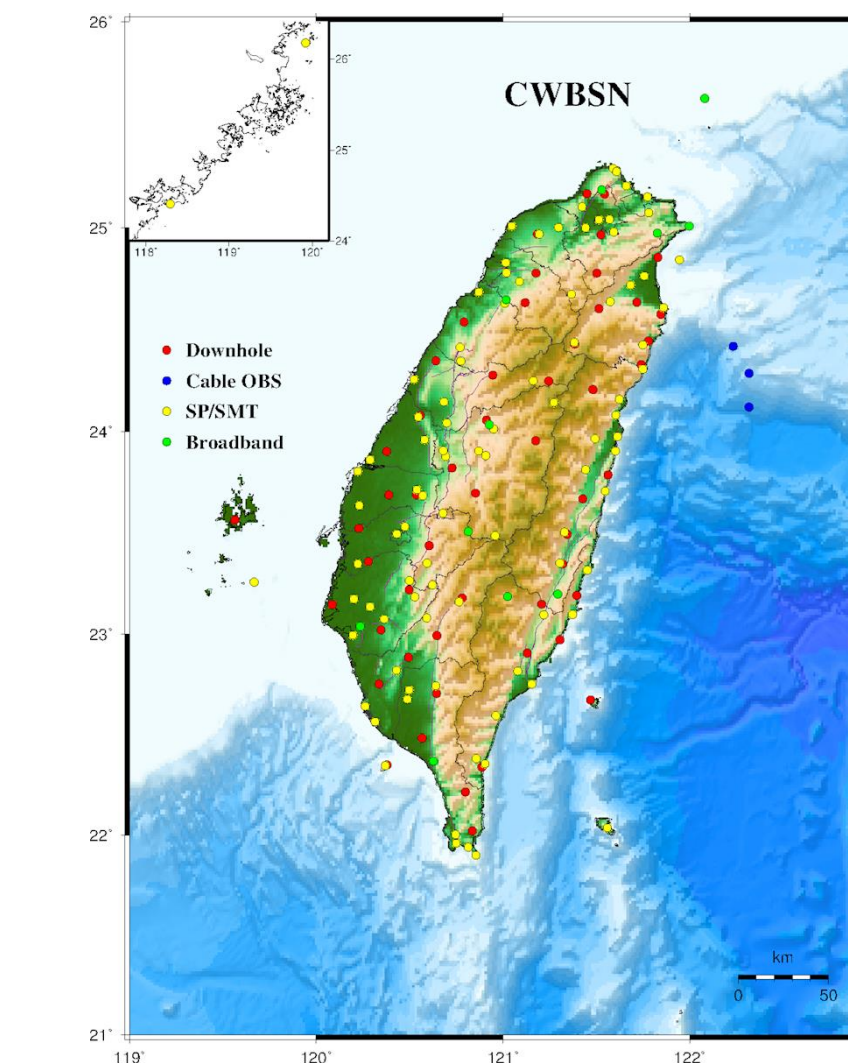
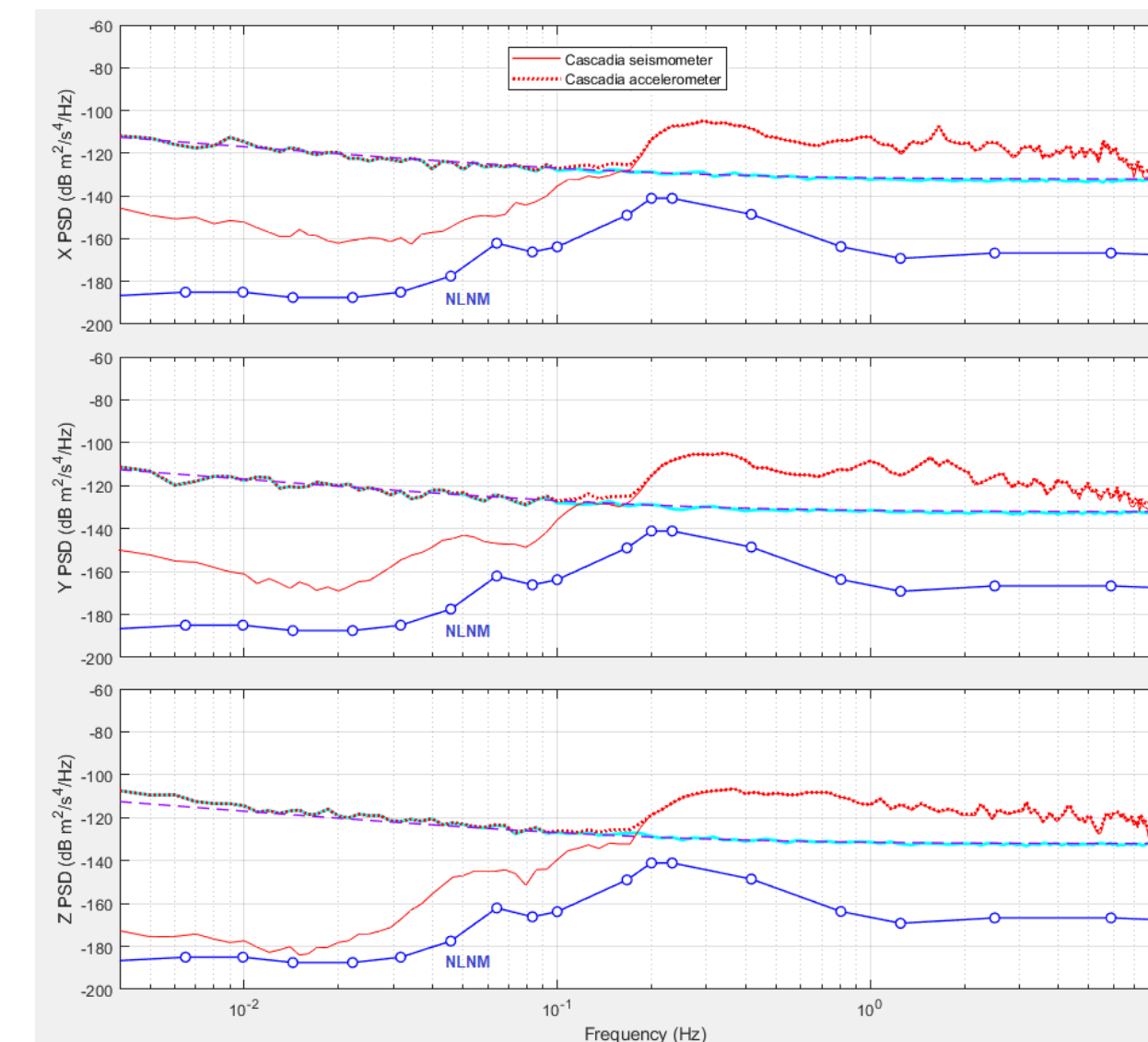


Figure 5: Acceleration PSD of background seismic signal and noncoherent noise at station SSPB (Xin Pi)



## Yilan Earthquake: Combining strong and weak motion data

Here we present data from Cascadia 120 Slim in the Taiwan CWB network, capturing a moderately large local earthquake (initial magnitude estimates ranged from M6.1 to M6.5) offshore near Yilan at 2021-10-24 5:11 UT. The amplitude of the earthquake signal varied with distance from the source to each receiver station. At many stations the signal was below the clip level (maximum output) of the Trillium weak-motion seismometer. However, for at least one station the peaks of the waveform were clipped on the seismometer output, so in that case the Titan strong-motion data can be used instead.

Figure 6 at right shows the raw counts waveform recorded at SSPB at 5:12:5-5:13 UT when signal from the Yilan earthquake arrived. This station was 260 km from the epicenter. The signal reached a peak of about 4e+5 counts (5% of full scale) on the weak motion seismometer system but produced a much smaller signal on the strong motion accelerometer system.

Figure 7 shows the same data after response correction, with both signals converted to units of acceleration. The waveforms overlay exactly, and the difference of the two signals (shown in green) appears as a flat line, meaning the signals are the same. The maximum amplitude of the difference signal is  $-1.7E-5 \text{ m/s}^2$ , versus  $-3.7E-3 \text{ m/s}^2$  for the corresponding acceleration peak, so the two signal amplitudes match within 0.46%.

Figure 8 shows the PSD of this acceleration data. The seismometer signal (solid red) and the accelerometer signal (dotted red) overlay precisely down to about 0.02 Hz (50 seconds period) where the signal from the earthquake drops below the accelerometer noise floor. The PSD of the difference signal (light blue line) still corresponds to the accelerometer system noise floor, meaning there is no difference in the two systems measurement of the earthquake signal. The earthquake signal peaks at nearly 60 dB above the noncoherent noise (difference signal), meaning the two measurements are 99.9% coherent.

At another station ILAB which was closer to Yilan, only 34 km from the epicenter of the earthquake, the signal amplitude was larger and reached the clip level of  $\pm 8E+6$  counts on the weak motion system, as shown in Figure 9. On the strong motion system it still appeared as a small signal, nowhere near full scale.

However when we view the same data in response-corrected acceleration (Figure 10), we can see that the acceleration measured by the strong motion system is larger, because it was not clipped - this represents the actual ground motion at the site. In other words, the strong motion system takes over when the weak motion system reaches its limit.

In conclusion, the Cascadia 120 Slim Posthole stations are fulfilling their intended purpose of delivering an integrated strong and weak motion dataset with full dynamic range and coherence, made possible by a precisely integrated strong and weak motion instrument.

Figure 6: Raw signal (digitizer counts) at SSPB showing earthquake arrival

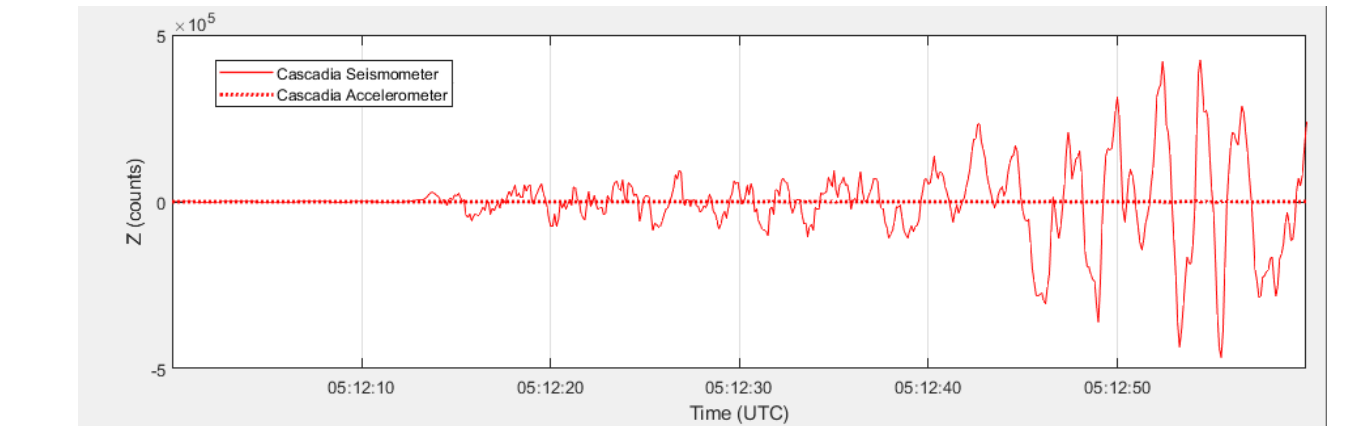


Figure 7: Response corrected acceleration at SSPB showing earthquake arrival

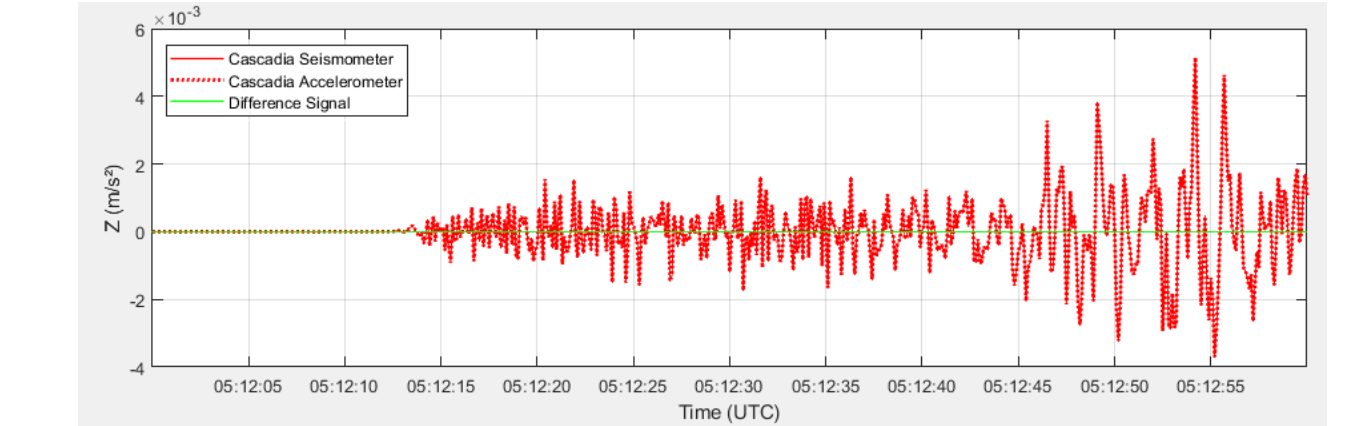


Figure 8: Acceleration PSD at SSPB during earthquake event

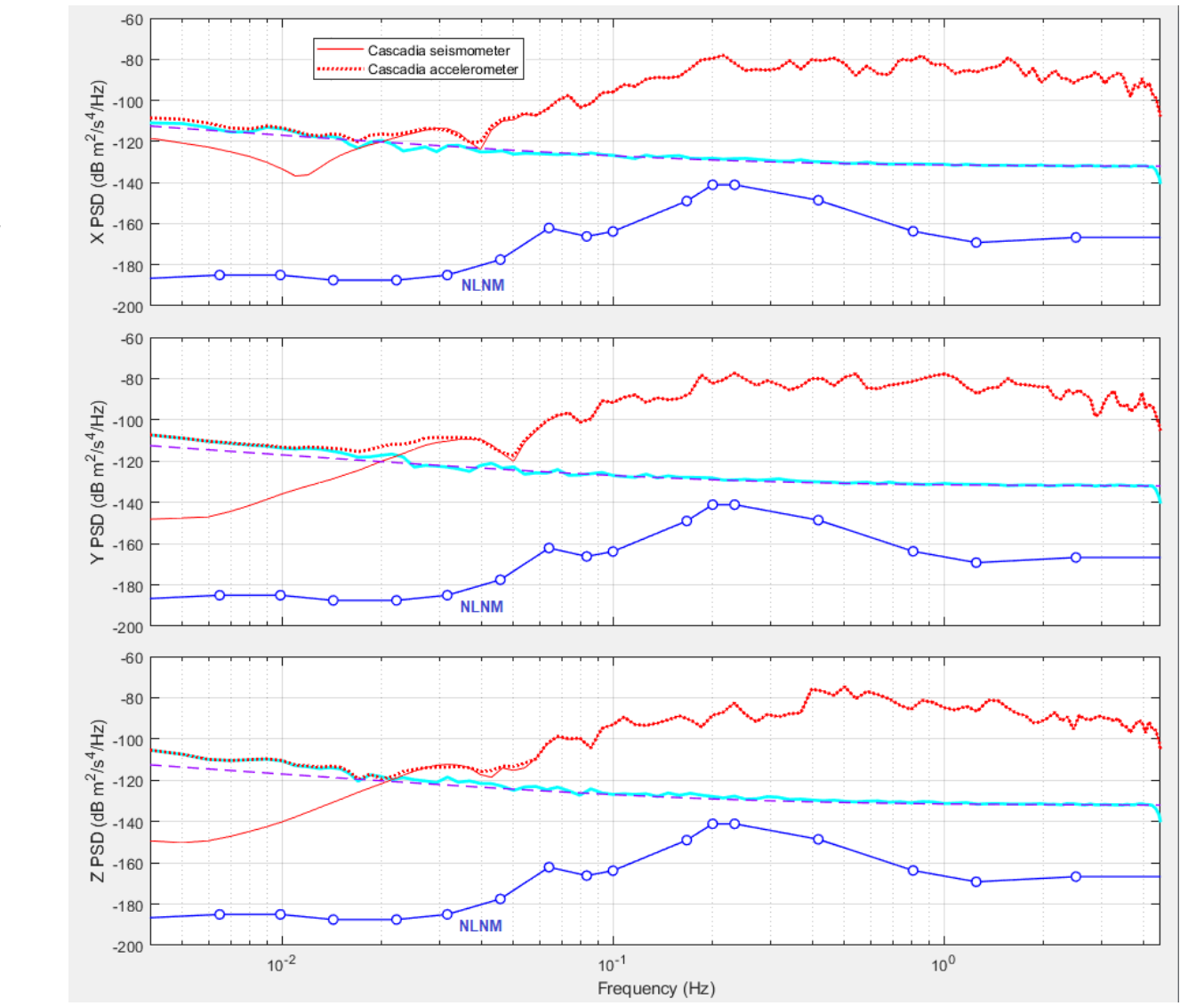


Figure 9: Raw signal (digitizer counts) at ILAB: earthquake clips seismometer

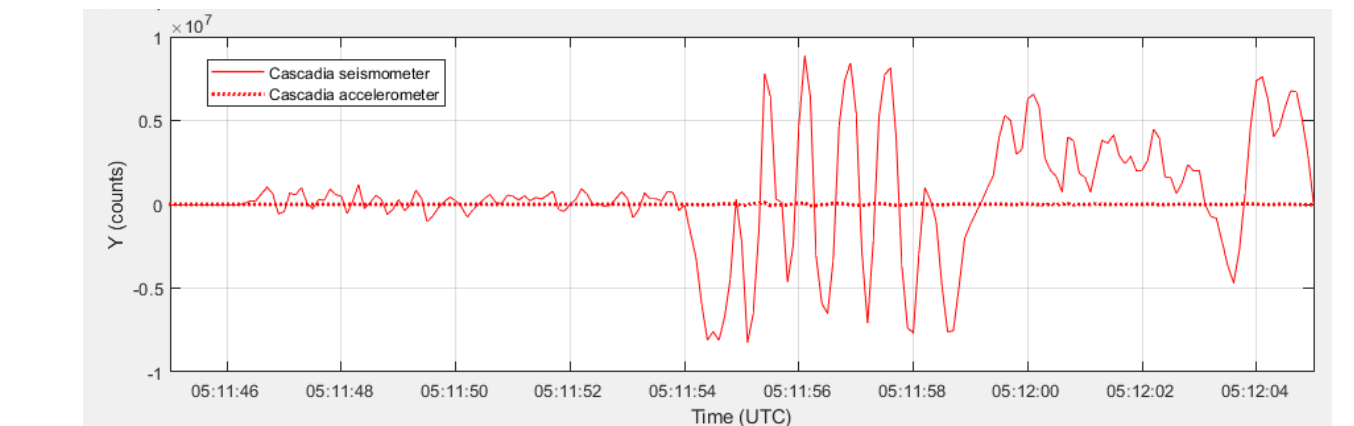
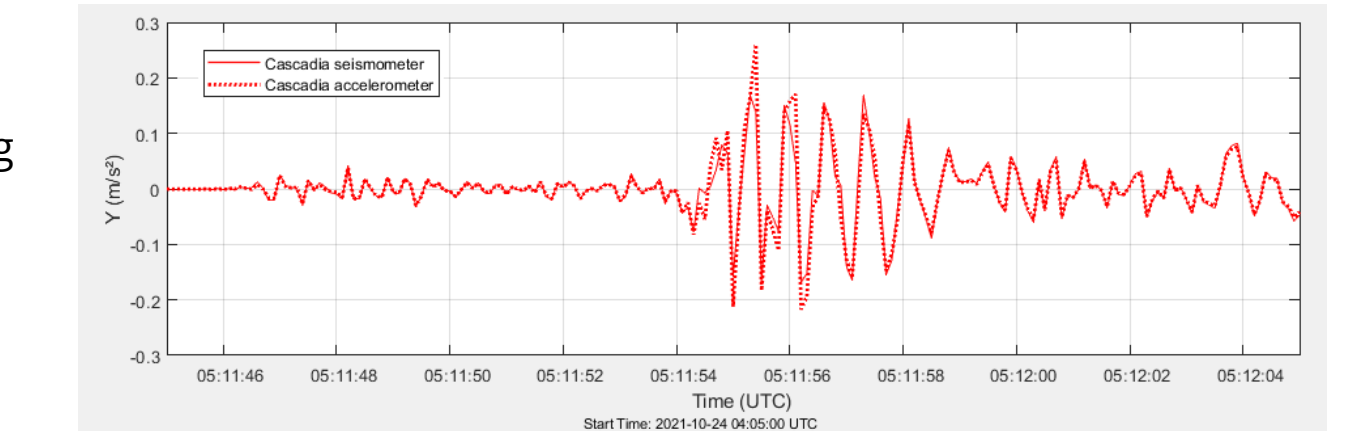


Figure 10: Response corrected acceleration at ILAB showing larger (unclipped) signal on strong-motion accelerometer



## REFERENCES

Holcomb, L. G. (1989). A Direct Method for Calculating Instrument Noise Levels in Side-by-Side Seismometer Evaluations, USGS Open-File Report 89-214, 34 pps.  
 Peterson, J. (1993). Observations and Modeling of Seismic Background Noise, USGS Open-File Report 93-322, 94 pps.  
 Sleeman, R., van Wietum, A. and Trampert, J. (2006) Three-Channel Correlation Analysis: A New Technique to Measure Instrumental Noise of Digitizers and Seismic Sensors, Bulletin of the Seismological Society of America, Vol. 96, No. 1, pp. 258-271.  
 Williams, T. & Austin, K. & Borsari, Adrian & Feaux, Karl & Jackson, Michael & Johnson, Wade & Mencin, David. (2010). Comparison of Deep Drill Braced Monument (DDBM) and Borehole Strainmeter (BSM) Wellhead GPS antenna mounts: a Plate Boundary Observatory (PBO) case study from Dinsmore, CA. AGU Fall Meeting Abstracts.